PROCEEDINGS OF SCIENCE

Measurement of Inclusive ep Cross Sections at High Q^2 at $\sqrt{s} = 225$ and 252 GeV and of the Longitudinal Proton Structure Function F_L at HERA

Stanislav Shushkevich*
on behalf of the H1 Collaboration
DESY Hamburg
E-mail: shushkev@mail.desy.de

Inclusive ep double differential cross sections for neutral current deep-inelastic scattering are measured with the H1 detector at HERA. The data were taken with a lepton beam energy of 27.6 GeV and two proton beam energies of $E_p = 460$ and 575 GeV corresponding to centre-of-mass energies of 225 and 252 GeV, respectively. The measurements cover the region of $6.5 \times 10^{-4} \leq x \leq 0.65$ for $35 \leq Q^2 \leq 800$ GeV^2 up to $y = 0.85$. The measurements are used together with previously published H1 data at $E_p = 920$ GeV and lower Q^2 data at $E_p = 460$, 575 and 920 GeV to extract the longitudinal proton structure function F_L in the region $1.5 \leq Q^2 \leq 800$ GeV^2.

XXII. International Workshop on Deep-Inelastic Scattering and Related Subjects,
28 April - 2 May 2014
Warsaw, Poland

*Speaker.

PoS(DIS2014)035

1. Introduction

The inclusive deep-inelastic (DIS) neutral current (NC) ep scattering cross section at moderate negative four-momentum transferred squared, Q^2, can be written in reduced form as [1]

$$\tilde{\sigma}_{\mathrm{NC}}(x,Q^2,y) = \frac{d^2\sigma_{\mathrm{NC}}}{dxdQ^2}\frac{xQ^4}{2\pi\alpha^2}\frac{1}{1+(1-y)^2} = F_2(x,Q^2) - \frac{y^2}{1+(1-y)^2}F_{\mathrm{L}}(x,Q^2), \tag{1.1}$$

where α denotes the fine structure constant, x is the Bjorken scaling variable and y is the inelasticity of the scattering process.

The reduced cross section is determined by two independent structure functions, F_2 and F_{L}. In Quark Parton Model F_2 represents the sum of the quark and anti-quark distributions weighted by the electric charges of quarks squared, and F_{L} is zero. In Quantum Chromodynamics (QCD) it differs from zero due to gluon and quark–antiquark pairs emissions.

The quantities x, Q^2 and y are connected by $sxy = Q^2$, where s is the centre-of-mass energy squared of the incoming electron and proton. Measurements of the differential cross sections at different values of $\sqrt{s}$ at fixed x and Q^2 provide an experimental separation of the F_2 and F_{L} structure functions. For this direct extraction of the structure functions data were taken at (reduced) proton beam energies of 460 and 575 GeV at the end of the HERA-II running. The lepton beam energy was kept at $E_e = 27.6$ GeV. These two datasets [2] are used together with the recently published data taken at $E_p = 920$ GeV [3] and low Q^2 data taken at $E_p = 460$, 575 and 920 GeV [4] to determine the structure functions F_2 and F_{L} in a model independent way. These data allow also for the measurement of the ratio $R = \sigma_L/\sigma_T = F_{\mathrm{L}}/(F_2 - F_{\mathrm{L}})$ of longitudinally σ_L and transversely σ_T polarised photon exchange cross section. In addition a direct local extraction of the gluon density $xg(x,Q^2)$ is performed.

2. Data Analysis

The measurements of the NC cross sections presented are performed in the range $35 \leq Q^2 \leq 800$ GeV^2, using e^+p data collected in two short dedicated data taking periods in 2007 in which the proton beam energy was reduced to 460 GeV and 575 GeV.

The measurements are performed with the positrons scattered into the acceptance of the Liquid Argon calorimeter (LAr), which corresponds to the polar angle range of the scattered positron $\Theta_e \lesssim 154^\circ$. The scattered positron is detected by searching for a compact and isolated electromagnetic energy deposition (cluster) in the LAr calorimeter.

As can be seen from Eq. (1.1) the contribution of F_{L} to the cross section is proportional to y^2 and thus significant only at high y. The most precise kinematic reconstruction method for $y \gtrsim 0.1$ is the e–method which relies solely on the cluster energy E'_e and Θ_e to reconstruct the kinematic variables Q^2, x and y as

$$Q^2_e = \frac{(E'_e \sin\Theta_e)^2}{1-y_e}, y_e = 1 - \frac{E'_e}{E_e}\sin^2\left(\frac{\Theta_e}{2}\right), x_e = \frac{Q^2_e}{sy_e} \tag{2.1}$$

Therefore the measurement at high y requires the measurement of the scattered positron with low energy. The photoproduction background increases rapidly with decreasing positron energy,

and the analysis is separated into two distinct regions: the nominal analysis ($y_e \leq 0.38$), and the high y analysis ($0.38 \leq y_e \leq 0.9$).

The nominal analysis follows the procedure described in [3]. In this region the minimum electron energy is kinematically restricted to be above 18 GeV. The photoproduction background is negligible, and the only sizable background contribution arises from remaining QED Compton events which is estimated using simulation and is statistically subtracted. The optimised treatment of the primary vertex determination and verification of the electron cluster with the help of tracker information provides the efficiency for ep interaction to be identified in the analysis larger than 99.5%.

In the high y region the analysis is extended down to energies of the scattered positron as low as 3 GeV. Dedicated techniques are used to reduce the background [5]. Cluster shape variables, and the ratio of the candidate electron cluster energy to the momentum of the associated track, are used in a neural network multilayer perceptron to discriminate signal from background. Additional information using the specific ionisation energy loss of the track, dE/dx, is also used to form a single electron discrimination variable D_{ele}, which is in use for the region $E'_e < 10$ GeV.

The scattered positron candidate is required to have positive charge corresponding to the beam lepton. The remaining background is estimated from the number of data events with opposite charge. This background is corrected to a charge asymmetry in photoproduction, which can arise due to the different detector response to particles compare to antiparticles, and is statistically subtracted from the positively charged sample.

Several common cuts are applied for both parts of the analysis. The quantity $E - P_z$ summed over all final state particles is required by energy-momentum conservation to be equal to twice electron beam energy for NC scattering in the absence of initial state radiation where the photon escapes undetected in the lepton beam direction. Restricting $E - P_z$ to be greater than 35 GeV considerably reduces the photoproduction background and suppresses events with hard initial state photon radiation. QED Compton events and non-ep events are suppressed using topological algorithms.

3. NC Cross Section and $F_{\mathrm{L}}(x, Q^2)$

The reduced cross sections $\tilde{\sigma}_{\mathrm{NC}}(x, Q^2)$ are measured in the kinematic range $35 \leq Q^2 \leq 800\,\mathrm{GeV}^2$ and $0.00065 \leq x \leq 0.65$ at two different reduced centre-of-mass energies and are referred to the LAr data. The data are shown in Fig. 1a together with previously published H1 data [3, 4]. The data are compared to QCD predictions based on the H1PDF 2012 fit [3] which provides a good description of the data.

According to Eq. (1.1) it is straightforward to determine F_{L} by a linear fit as a function of $f(y) = y^2/(1+(1-y)^2)$ to the reduced cross section measured at given values of x and Q^2 but at different centre-of-mass energies. However to properly account for correlations across all measurements the alternative procedure is applied. The structure functions F_{L} and F_2 are simultaneously determined from the cross section measurement using a χ^2 minimisation technique as employed

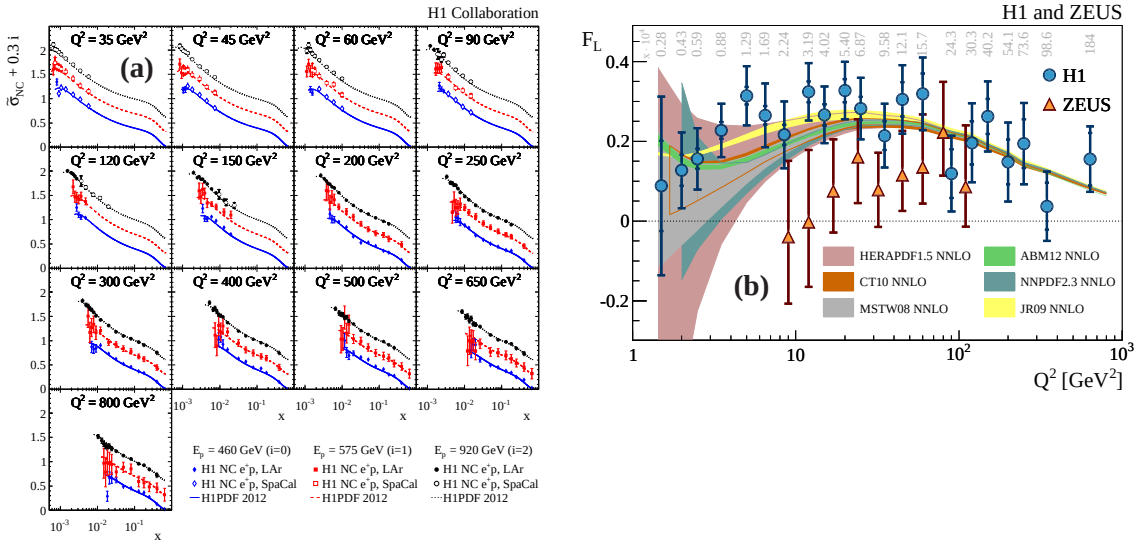

Figure 1: **(a)** Reduced cross section $\tilde{\sigma}_{\rm NC}(x,Q^2)+0.3i$ measured at three proton beam energies $E_p =$ 460 GeV, 575 GeV and 920 GeV displaced vertically for better visibility as a function of x at fixed values of Q^2. The curves represent the prediction from the H1PDF2012 NLO QCD fit. **(b)** Proton structure function $F_{\rm L}$ averaged over x at different Q^2 bins. The data are compared to NNLO predictions from a selection of PDF sets as indicated.

in [4]. The χ^2 function for the minimisation is

$$\chi^2(F_{L,i},F_{2,i},b_j)=\sum_i \frac{\left[(F_{2,i}-f(y)F_{L,i})-\sum_j \Gamma_{i,j}b_j-\mu_i)\right]^2}{\Delta_i^2}+\sum_j b_j^2, \tag{3.1}$$

where μ_i is the measured reduced cross section at an x,Q^2 point i with the combined statistical and uncorrelated systematic uncertainty $\Delta_i=\sqrt{\Delta_{i,stat}^2+\Delta_{i,syst}^2}$. The effect of correlated error sources j on the cross section measurement is given by the systematic error matrix $\Gamma_{i,j}$. The technique reduces to the linear fit when considering a single x,Q^2 bin and neglecting correlations between the cross section measurements. The χ^2 per degree of freedom is found to be $184/210$.

In order to reduce the experimental uncertainties the $F_{\rm L}$ measurements are combined at each Q^2 value, and the two highest Q^2 bins are also averaged. The resulting data is shown in Fig. 1b together with the ZEUS measurement [6]. A probability of consistency of the H1 and ZEUS measurements is 20%. The data are compared to a suite of QCD predictions at NNLO: HERAPDF1.5 [7], CT10 [8], ABM11 [9], MSTW2008 [10], JR10 [11] and NNPDF2.2 [12]. The perturbative calculations provide a reasonable description of the data.

The cross section ratio R of longitudinally to transversely polarised virtual photons are determined by minimising the χ^2 function of Eq. (3.1) where $F_{\rm L}$ is replaced by $F_{\rm L}=\frac{R}{1+R}F_2$ assuming R is constant as a function of x for a given value of Q^2. The resulting value of $R(Q^2)$ in shown in Fig. 2b together with the ZEUS data. The result is compared with the prediction of the HERAPDF1.5 NNLO for $\sqrt{s}=225$ GeV and $y=0.7$. The fit is repeated by assuming that R is constant across the entire Q^2 range and yields a value of $R=0.23\pm0.04$ with $\chi^2/ndf=314/367$.

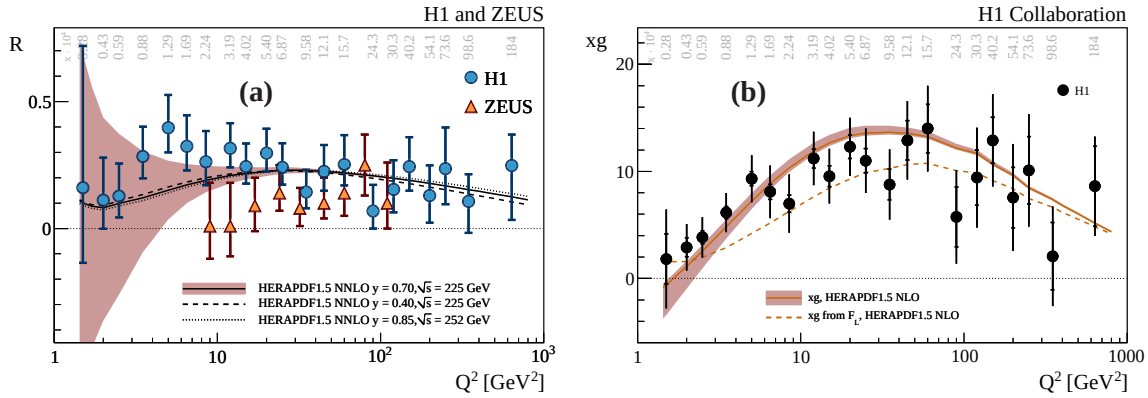

Figure 2: **(a)** Ratio $R(Q^2)$ averaged over x together with the prediction from the HERAPDF1.5 NNLO QCD fit. **(b)** Gluon density $xg(x,Q^2)$ averaged over x. The shaded regions represent the prediction from the HERAPDF1.5 NLO QCD fit. The dashed line corresponds to xg obtained from the F_{L} prediction based on the HERAPDF1.5 NLO QCD fit.

At order α_s the gluon density is related to F_{L} via the approximate relation [13, 14]

$$xg(x,Q^2) \approx 1.77 \frac{3\pi}{2\alpha_s(Q^2)} F_{\mathrm{L}}(x,Q^2). \tag{3.2}$$

The direct measurement of F_{L} is used to demonstrate its sensitivity to the gluon density obtained from a NLO QCD fit to DIS data. In Fig. 2b the gluon density extracted according to the relation (3.2) is compared to the prediction from the gluon density determined in the NLO HERAPDF1.5 QCD fit [7]. To judge on the goodness of the approximation the gluon density as obtained by applying the same relation to the F_{L} prediction based on NLO HERAPDF1.5 QCD fit is also shown. A reasonable agreement between the gluon density as extracted from the direct measurement of F_{L} based on the approximate relation with the gluon derived indirectly from scaling violations is observed.

4. Summary

The neutral current inclusive DIS cross section for ep interactions are measured at two centre-of-mass energies of $\sqrt{s} = 225$ and 252 GeV. The measurements are performed up to the highest accessible inelasticity $y = 0.85$ where the contribution of the F_{L} structure function to the reduced cross section is sizable. The F_{L} and F_2 structure functions are simultaneously extracted in a model independent way using the data together with previously published measurements at $\sqrt{s} = 319$ GeV. The ratio R of the longitudinally to transversely polarised virtual photon cross section is measured and consistent with being constant over the kinematical range of the data, and is determined to be equal to 0.23 ± 0.04. A gluon density is extracted based on NLO approximation from the F_{L} measurement. Good agreement is observed between the measurements and perturbative QCD calculations at NNLO.

References

[1] E. Perez and E. Rizvi, Rep. Prog. Phys. **76** (2013) 046201 [arXiv:1208.1178].

[2] V. Andreev *et al.* [H1 Collaboration], Eur. Phys. J. C **74** (2014) 2814 [arXiv:1312.4821].

[3] F. D. Aaron *et al.* [H1 Collaboration], JHEP **1209** (2012) 061 [arXiv:1206.7007].

[4] F. D. Aaron *et al.* [H1 Collaboration], Eur. Phys. J. C **71** (2011) 1579 [arXiv:1012.4355].

[5] F. D. Aaron *et al.* [H1 Collaboration], Eur. Phys. J. C **72** (2012) 2148 [arXiv:1206.4346].

[6] DESY-14-053, submitted to Phys. Lett. B [arXiv:1404.6376].

[7] H1 and ZEUS Collaborations, H1prelim-13-141, ZEUS-prel-13-003, http://www-h1.desy.de/h1/www/publications/htmlsplit/H1prelim-13-141.long.html

[8] H.-L. Lai *et al.*, Phys. Rev. D **82** (2010) 074024 [arXiv:1007.2241].

[9] S. Alekhin, J. Blümlein and S. Moch, [arXiv:1310:3059].

[10] A. D. Martin *et al.*, Eur. Phys. J. **C63** (2009) 189 [arXiv:0901.0002].

[11] M. Gluck, P. Jimenez-Delgado and E. Reya, Eur. Phys. J. C **53** (2008) 355 [arXiv:0709.0614]; P. Jimenez-Delgado and E. Reya, Phys. Rev. D **79** (2009) 074023 [arXiv:0810.4274].

[12] R. D. Ball *et al.*, Nucl. Phys. B **867** (2013) 244 [arXiv:1207.1303]; S. Forte *et al.*, Nucl. Phys. B **834**, 116 (2010) [arXiv:1001.2312].

[13] A. M. Cooper-Sarkar *et al.*, Z. Phys. C **39** (1988) 281.

[14] E. B. Zijlstra and W. L. van Neerven, Nucl. Phys. B **383** (1992) 525.

PoS(DIS2014)035